



AFRL-RX-TY-TP-2011-0057

BACTERIAL SUNSCREEN: LAYER-BY-LAYER DEPOSITION OF UV-ABSORBING POLYMERS ON WHOLE-CELL BIOSENSORS (POSTPRINT)

D. Matthew Eby, Randi N. Tatum and Karen E. Farrington
Universal Technology Corporation
1270 Fairfield Road
Dayton, OH 45432

Svetlana Harbaugh and Nancy Kelley-Loughnane
Human Effectiveness Directorate
Air Force Research Laboratory
2510 Fifth Street
Wright-Patterson Air Force Base, OH 45433-7913

Glenn R. Johnson
Airbase Technologies Division
Air Force Research Laboratory
139 Barnes Drive, Suite 2
Tyndall Air Force Base, FL 32403-5323

Contract No. FA4819-11-C-0003

February 2012

DISTRIBUTION A: Approved for public release; distribution unlimited.
88ABW-2012-0749, 14 February 2012.

**AIR FORCE RESEARCH LABORATORY
MATERIALS AND MANUFACTURING DIRECTORATE**

REPORT DOCUMENTATION PAGE					Form Approved OMB No. 0704-0188	
The public reporting burden for this collection of information is estimated to average 1 hour per response, including the time for reviewing instructions, searching existing data sources, gathering and maintaining the data needed, and completing and reviewing the collection of information. Send comments regarding this burden estimate or any other aspect of this collection of information, including suggestions for reducing the burden, to Department of Defense, Washington Headquarters Services, Directorate for Information Operations and Reports (0704-0188), 1215 Jefferson Davis Highway, Suite 1204, Arlington, VA 22202-4302. Respondents should be aware that notwithstanding any other provision of law, no person shall be subject to any penalty for failing to comply with a collection of information if it does not display a currently valid OMB control number.						
PLEASE DO NOT RETURN YOUR FORM TO THE ABOVE ADDRESS.						
1. REPORT DATE (DD-MM-YYYY) 01-FEB-2012		2. REPORT TYPE Journal Article POSTPRINT		3. DATES COVERED (From - To) 14-NOV-2010 -- 14-NOV-2011		
4. TITLE AND SUBTITLE Bacterial Sunscreen: Layer-by-Layer Deposition of UV-Absorbing Polymers on Whole-Cell Biosensors (POSTPRINT)				5a. CONTRACT NUMBER FA4819-11-C-0003		
				5b. GRANT NUMBER		
				5c. PROGRAM ELEMENT NUMBER		
6. AUTHOR(S) ^Eby, D. Matthew; *Harbaugh, Svetlana; ^Tatum, Randi N.; ^Farrington, Karen E.; *Kelley-Loughnane, Nancy; **Johnson, Glenn R.				5d. PROJECT NUMBER		
				5e. TASK NUMBER		
				5f. WORK UNIT NUMBER QL102007		
7. PERFORMING ORGANIZATION NAME(S) AND ADDRESS(ES) ^Universal Technology Corporation, 1270 North Fairfield Road, Dayton, OH 45432; *Human Effectiveness Directorate, 2510 Fifth Street, Wright-Patterson Air Force Base, OH 45433-7913				8. PERFORMING ORGANIZATION REPORT NUMBER		
9. SPONSORING/MONITORING AGENCY NAME(S) AND ADDRESS(ES) **Air Force Research Laboratory Materials and Manufacturing Directorate Airbase Technologies Division 139 Barnes Drive, Suite 2 Tyndall Air Force Base, FL 32403-5323				10. SPONSOR/MONITOR'S ACRONYM(S) AFRL/RXQL		
				11. SPONSOR/MONITOR'S REPORT NUMBER(S) AFRL-RX-TY-TP-2011-0057		
12. DISTRIBUTION/AVAILABILITY STATEMENT Distribution Statement A: Approved for public release; distribution unlimited.						
13. SUPPLEMENTARY NOTES Ref Public Affairs Case # 88ABW-2012-0749, 14 February 2012. Document contains color images. Published in Langmuir, 2012, 28 (28), pp 10521-10527. DOI: 10.1021/la3014514						
14. ABSTRACT UV-protective coatings on live bacterial cells were created from the assembly of cationic and UV-absorbing anionic polyelectrolytes using layer-by-layer (LbL) methodology. A cationic polymer (poly-allylamine) and three different anionic polymers with varying absorbance in the UV range (poly-vinyl sulfate, poly-4-styrenesulfonic acid, and humic acid) were used to encapsulate <i>E. coli</i> cells expressing green fluorescent protein (GFP) either constitutively or through a theophylline-inducible riboswitch. Riboswitches are regulatory elements that activate gene expression after a ligand-RNA binding event; hence, they operate as a cellular biosensor that will express a reporter protein after exposure to a ligand target. <i>E. coli</i> cells coated with polymers absorbing in the far UV range demonstrated enhanced protection to GFP stability, metabolic activity, and viability after prolonged exposure to radiation from a germicidal lamp. The results show the effectiveness of LbL coatings to provide enhanced protection to living cells for use in biosensor technology.						
15. SUBJECT TERMS layer-by-layer, UV-radiation, sunscreen, whole-cell biosensor, applied microbiology						
16. SECURITY CLASSIFICATION OF:			17. LIMITATION OF ABSTRACT	18. NUMBER OF PAGES	19a. NAME OF RESPONSIBLE PERSON	
a. REPORT	b. ABSTRACT	c. THIS PAGE			Glenn R. Johnson	
U	U	U	UU	7	19b. TELEPHONE NUMBER (Include area code) 850 283 6062	

Reset

Bacterial Sunscreen: Layer-by-Layer Deposition of UV-Absorbing Polymers on Whole-Cell Biosensors

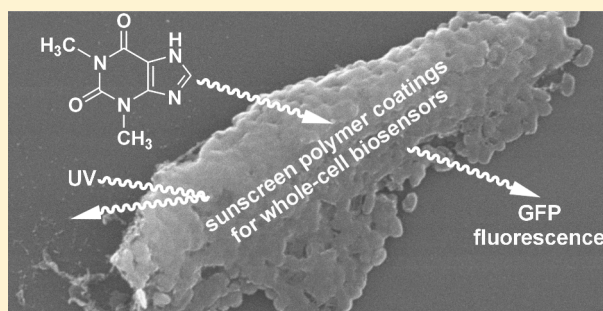
D. Matthew Eby,^{*,†,‡} Svetlana Harbaugh,[§] Randi N. Tatum,^{†,‡} Karen E. Farrington,^{†,‡} Nancy Kelley-Loughnane,[§] and Glenn R. Johnson^{*,‡}

[†]Universal Technology Corporation and [‡]Air Force Research Laboratory, Materials and Manufacturing Directorate, Tyndall Air Force Base, 139 Barnes Drive, Building 1117, Tyndall AFB, Florida 32403, United States

[§]Air Force Research Laboratory, 711th Human Performance Wing, Human Effectiveness Directorate, Wright-Patterson Air Force Base, Wright-Patterson AFB, Ohio 45433, United States

S Supporting Information

ABSTRACT: UV-protective coatings on live bacterial cells were created from the assembly of cationic and UV-absorbing anionic polyelectrolytes using layer-by-layer (LbL) methodology. A cationic polymer (polyallylamine) and three different anionic polymers with varying absorbance in the UV range (poly(vinyl sulfate), poly(4-styrenesulfonic acid), and humic acid) were used to encapsulate *Escherichia coli* cells with two different green fluorescent protein (GFP) expression systems: constitutive expression of a UV-excitable GFP (GFPuv) and regulated expression of the intensely fluorescent GFP from amphioxus (GFPa1) through a theophylline-inducible riboswitch. Riboswitches activate protein expression after specific ligand–RNA binding events. Hence, they operate as a cellular biosensor that will activate reporter protein synthesis after exposure to a ligand target. *E. coli* cells coated with UV-absorbing polymers demonstrated enhanced protection of GFP stability, metabolic activity, and viability after prolonged exposure to radiation from a germicidal lamp. The results show the effectiveness of LbL coatings to provide UV protection to living cells for biotechnological applications.



INTRODUCTION

UV radiation from prolonged exposure to sunlight is a bane to all organisms. Yet, all organisms, either directly or indirectly, rely on sunlight for vitality and nourishment. In the microbiota, most aerobic microorganisms require chemical protection or behavior modifications to protect against UV radiation.¹ For example, algae and cyanobacteria synthesize carotenoid pigments and mycosporine-like amino acids that absorb in the UV range and can quench UV-induced intracellular free radicals.^{2,3} Common in both microorganisms and higher organisms, melanin production provides a natural sunscreen, due to absorption of UV radiation by the polyaromatic structure.⁴ In addition to chemical protection, microbes utilize specific behaviors to attenuate exposure to sunlight. Motile microorganisms can move away from areas of high light intensity and can aggregate into biofilms and synthesize exopolymers that block UV light.⁵ Without these mechanisms, UV radiation produces reactive oxygen species and induces excessive DNA strand breakage and denaturation, which leads to cell damage and dramatic increases in genetic mutations.¹

Natural adaptations for UV protection are not sufficient for microorganisms used in biotechnological applications that operate in direct sunlight or in environments where harmful UV light is usually absorbed by the atmosphere (e.g., nonaqueous and astrobiological applications). Developing

biomimetic approaches to enhance UV radiation protection for microorganisms has several advantages, particularly for use with whole-cell biosensors.⁵ Microbial biosensors are a promising technology due to their excellent specificity, sensitivity, portability, and regenerative capabilities.⁶ However, as living entities, recombinant microorganisms are more complex and fragile than conventional sensor devices and can be more sensitive to harsh environmental conditions. In particular, recombinant or natural microorganisms that harbor useful biotechnology applications may not be adapted to the operational environment. Prolonged exposure to ambient sunlight intensity can be lethal to microorganisms lacking natural properties or physical mechanisms to protect against UV radiation.^{7,8} Consequently, methods to successfully apply protective mechanisms to engineered microbes for biotechnology are warranted and, at the same time, must not affect the utility of the microorganism.

Polyelectrolytic layering (i.e., layer-by-layer or LbL) of biocompatible polymers provides a convenient method to enhance cells with new protective and functional properties.^{9,10} LbL coatings are interconnected through noncovalent,

Received: April 9, 2012

Revised: June 11, 2012

Published: June 13, 2012



Coulombic interactions, which permit the coatings to be flexible and mimic the fluidic movements of cellular plasma membranes and also allow the diffusion of molecules essential to cellular function. In most cases, LbL layering can be completed in physiological solutions and at conditions that preserve the viability of cells. The procedure has been successfully completed on mammalian cells, microorganisms, and spores.^{11–18} Coatings can provide protective properties, alter the charge of the cellular surface, decorate the cell with artificial recognition elements, or hide existing antigens.^{19–21} Hence, polyelectrolytes that absorb UV radiation can be employed as a “sunscreen” coating on the surface of bacterial cells for enhanced protection against UV-related damage.

Herein, a method to coat bacterial cell-based biosensors with UV-absorbing polymers was devised that uses polyelectrolytic LbL techniques. The cellular biosensor is an *Escherichia coli* engineered with the riboswitch-dependent expression of the intensely fluorescent GFPa1 from amphioxus and activated by theophylline.^{22–25} Riboswitches (RNA switches) are post-transcriptional regulatory elements that control protein expression after a ligand–RNA binding event.²⁶ Riboswitches sense their target ligand through binding to an inclusive aptamer domain, and the resulting complex adopts a conformational change to ultimately unlock protein expression. Hence, they operate as a cellular biosensor that will synthesize a reporter protein after exposure to a target molecule. An artificial riboswitch was devised utilizing a theophylline-binding aptamer to efficiently control translation dependent on a small molecule ligand in vivo.^{23,24} This sensing platform has been adopted in a variety of biotechnological applications.^{22,27–35}

A first set of experiments was devised to assess the protective properties of different UV-absorbing cellular coatings on protein stability, metabolic activity, and viability. *E. coli* cells constitutively expressing the gene for a UV-excitable GFP (GFPuv) were coated with oppositely charged polymers with various UV absorbance characteristics. Coated and uncoated cells were then exposed to UV light and monitored for GFPuv stability, metabolic activity, and viability. In a second set of experiments, *E. coli* cells with a riboswitch post-transcriptional activator for GFPa1 gene expression were immobilized as a monolayer onto the surface of microplate wells and coated in polyelectrolyte layers. Riboswitch cells were exposed to UV light and monitored for their ability to respond to the transcriptional regulator theophylline and increase expression of GFPa1.

■ EXPERIMENTAL SECTION

Bacterial Strains, DNA Manipulations, and Culture Conditions. *E. coli* cells used in this study were R34 containing pGFPuv (Clontech Inc., Mountain View, CA) and BL21 containing pSAL:RS12.1GFPa1His. In the latter genetic construct, DNA encoding the theophylline synthetic riboswitch RS12.1²⁴ was placed upstream of the GFPa1 gene within pSAL vector, as similarly constructed for the tobacco etch virus (TEV) protease expression described in Harbaugh et al.²² Electroporation of cells for transformation of plasmids and other DNA manipulations were completed as described in Sambrook et al.³⁶ Cells were typically grown at 37 °C with shaking at 225 rpm in Luria–Bertani broth (LB) containing 100 mg L⁻¹ ampicillin.³⁰ For UV exposure and control activity assays, a defined medium was used containing M9 mineral salts supplemented with 0.1% casamino acids and 0.008% glycerol.³⁴ The reduced glycerol and casamino acid concentrations in the assay media will support protein synthesis but limit cell replication. For assays containing theophylline, a theophylline stock solution (100 mM) in DMSO was diluted into assay media to a final concentration of 2.5 mM. UV

exposure assays using R34(pGFPuv) were completed in 6-well microtiter plates (Corning Inc., Corning, NY). UV exposure assays using BL21(pSAL:RS12.1GFPa1His) were completed in 12-well poly(D-lysine)-coated microtiter plates (Biocoat, Becton Dickinson, Bedford, MA).

Chemicals. Poly(vinyl sulfate) (PVS, typical M_w = 170 000), sodium poly(styrenesulfonate) (PSS, typical M_w = 70 000), poly(allylamine hydrochloride) (PAH, typical M_w = 15 000), and humic acid (HA) were all obtained from Sigma–Aldrich (St. Louis, MO). Final concentrations of all polyelectrolyte solutions were 2 mg mL⁻¹ in 0.85% saline except for HA, which was used at a saturating concentration (~0.5 mg mL⁻¹). The pH of the PVS solution was raised to 6 using NaOH. Amine-functionalized latex beads (100 nm mean particle diameter, Sigma–Aldrich) were diluted in 0.85% saline (0.25%, solids) before use. All other reagents were from Sigma–Aldrich unless noted otherwise.

LBL Assembly on R34(pGFPuv) Cell Surfaces. Cells from a 50 mL overnight culture were harvested by centrifugation for 5 min at 4500g at 4 °C (5810R centrifuge, Eppendorf, Hamburg, Germany) and the supernatant was discarded. Cells were washed three times by resuspending the pellet in 10 mL 0.85% saline solution and repeating the centrifugation step (wash step). The first polyelectrolyte layer was added by resuspending the cell pellet in 10 mL of PAH. The pellet was incubated in PAH for 1 min and then centrifuged as stated above. The supernatant was discarded, and the cells were washed twice before the next polyelectrolyte layer was added. The second layer was formed by suspending the pellet in 10 mL of an anionic polyelectrolyte for 1 min. The entire procedure was repeated until cells had two layers of PAH and two layers of the anionic polyelectrolyte. Uncoated cells were prepared in the same manner except 0.85% saline replaced all polyelectrolyte solutions. All samples and layering solutions were kept on ice throughout the LbL assembly, and cells were stored at –20 °C until used in assays. Before completing assays, cell pellets were thawed and washed once as described above to remove any debris from lysed cells. To validate the efficiency of the layering procedure, amine-functionalized latex beads were added as a final coat using the same procedure described above and prepared for scanning electron microscopy (SEM) using methods described in the following section.

Polyelectrolyte Layering Characterization. UV–vis spectra of polyelectrolytes were collected using a Cary 3E spectrophotometer (Varian Inc., Palo Alto, CA). The surface potential of coated cells in solution was determined using a Zetasizer Nano CZ90 (Malvern Instruments Ltd., Worcestershire, U.K.). Surface charge was measured by electrophoretic mobility coupled with laser Doppler velocimetry and calculated as the ζ potential. Analysis was completed at 25 °C, and each reported measurement was an average of at least six independent samples and between 12 and 20 measurements of each sample. Atomic force microscopy (AFM) images were obtained using a Nanoscope V, equipped with a Multimode V scanning probe microscope and a PicoForce stage (Bruker AXS Inc., Madison, WI). After the coating procedure, cells were resuspended in ultrapure water and a drop of the suspension was placed on a silicon wafer surface and air-dried for 5 min. Images were acquired in tapping mode using a type RTESP probe (Bruker AXS). The edge height of cells was measured from amplitude images as the distance from the sample substrate surface to the first plateau found on the cell surface. At least nine measurements from at least three separate cells were used in calculation of the edge height average and standard deviation. For SEM, cells were resuspended in ultrapure water and a drop of the suspension was placed on an aluminum coupon surface. Samples were air-dried for 5 min and incubated for at least 2 h in glutaraldehyde (2.5% in 0.1 M cacodylate buffer). After glutaraldehyde treatment, cells were dehydrated by incubating in increasing concentrations of ethanol (50%, 70%, 80%, 90%, and 100%) for 10 min each. After dehydration, the *E. coli* cells were dried in an Autosamdri-815 critical point dryer according to the manufacturer's instructions (Tousimis Research Corporation, Rockville, MD). A Desk V sputter coater (Denton Vacuum, Inc., Moorestown, NJ) was utilized for 30 s to coat the cells in gold. Images were captured with a Hitachi S 2600N SEM (Hitachi High Technologies America, Inc., Pleasanton, CA).

LbL Assembly on BL21(pSAL:RS12.1GFPa1His) Cells Adsorbed to Microplate Well Surfaces. Overnight cultures were diluted 1:100 in LB and incubated in 12-well microplates coated with poly(D-lysine) (2 mL in each well) for 4 h at 37 °C without shaking. The growth medium was removed from the wells, and each well was washed with 0.85% saline three times to remove trace amounts of media. Successive layers were coated onto attached cells in the well by first adding 1 mL of the PAH solution described above and then removing and adding the anionic polyelectrolyte solution with two 1 mL washes of 0.85% saline in between each layer. Cells were incubated in each layer for 2 min. For uncoated cells, 0.85% saline replaced polyelectrolyte solutions in the above method. Cells were then used immediately in assays.

UV Exposure and Sensitivity Measurement Assays. For assays using R34(pGFPuv), six-well microtiter plates containing 5 mL of uncoated or coated cells in assay buffer were placed in a biological safety cabinet (Forma Class II, A2, Thermo Scientific) with the germicidal lamp turned on (Phillips 30W G30T8 UV bulb). The bulb emits short-wave UV radiation centered at 254 nm (UVC). At set intervals, plates were removed from the cabinet and fluorescence was measured with emission and excitation wavelengths of 390 and 508 nm, respectively. In addition, 50 μ L of each cell suspension was added to 50 μ L of BacTiter-Glo Reagent in a 96-well microtiter plate and relative ATP concentration was measured by luminescence according to the manufacturer's instruction (Promega Corp., Madison, WI). UV/visible spectrophotometry was completed using a Synergy 4 microplate reader (Biotek Inc., Winooski, VT). Viability was determined by sampling the assay cultures at set intervals and plating serial dilutions on LB solid media with ampicillin (100 mg L⁻¹). Colony forming units (CFU) were enumerated after overnight incubation (37 °C).

For UV sensitivity assays using BL21(pSAL:RS12.1GFPa1His), 12-well microplates containing adsorbed uncoated and coated cells and 1 mL of theophylline assay buffer were exposed to UV radiation as described above. Fluorescence was measured with an excitation and emission wavelength of 480 and 510 nm, respectively. Kinetic data were calculated using *GenS* software (BioTek Inc.). Kinetic variables were calculated as follows: V_{\max} , maximal change in relative fluorescence units (RFU) over time; $t_{V_{\max}}$, time at V_{\max} ; t_{lag} , lag time defined by the time interval between the line of maximum slope of the propagation phase and the RFU baseline; $\text{RFU}_{V_{\max}}/\text{RFU}_0$, fold RFU increase at $t_{V_{\max}}$ over RFU at start of assay.

RESULTS

UV Sensitivity of Coated and Uncoated Cells in Solution. R34(pGFPuv) was coated in sequential layers of cationic PAH and anionic PVS, PSS, or HA to assess the ability of each anionic polymer to protect cells from UV radiation. Figure 1 shows the general structure and absorbance of the polyelectrolytes in the UV/visible range. R34(pGFPuv) was coated with a total of four layers, two with PAH and two with the anionic polymer, and successful layering was monitored by measuring the zeta potential (Figure 2). Significant aggregation of cells was observed after polyelectrolyte layering, which was not present with cells exposed only to saline (Figure 3). Uncoated cells appeared homogeneous in suspension and were easily seen in SEM images as individual cells. Alternatively, in coated cell preparations, aggregation was visible to the naked eye and SEM of coated cells showed aggregates containing hundreds to thousands of cells. A representative AFM image is presented in Figure 4. AFM analysis reveals that the cells remain intact after the coating procedure and appear to have a complete coating of polyelectrolytic layers, despite the aggregation shown in SEM images that suggested cells may not have received an even coat of polyelectrolytes. AFM images of uncoated cells show features within the cell, while the features of coated cells are masked by the coatings. In addition, coated cells appear to have a thicker cell envelope. During the

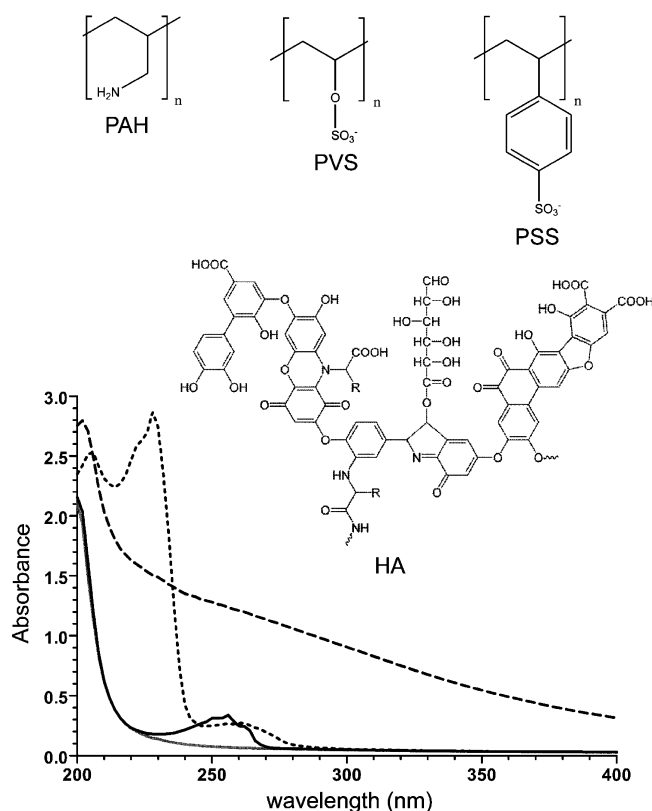


Figure 1. Top: Structure of poly(allylamine) (PAH), poly(vinyl sulfate) (PVS), poly(4-styrenesulfonic acid) (PSS), and a typical structure of humic acid (HA). Bottom: UV/visible spectra of PAH (gray line), PVS (black line), PSS (dotted line), and HA (dashed line).

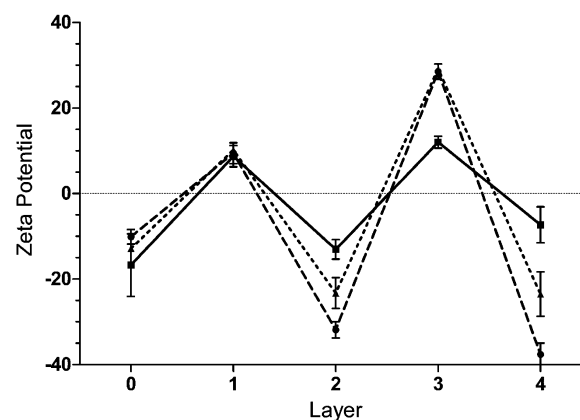


Figure 2. ζ potential of successive polyelectrolyte layering on R34(pGFPuv) cells using PAH for layers 1 and 3 and PVS (solid), PSS (dash), and HA (dotted) for layers 2 and 4.

sample drying process for AFM imaging in air, cells flatten and the cell envelope will extend beyond the cell body and laminate to the sample substrate surface. The amplitude images shown do not show actual height, so the corresponding height image was used to measure the cell edges (see the Supporting Information). The edge thicknesses of laminated cells were measured from the corresponding AFM height images, and the average edge height was 15.6 ± 4.5 nm and 40.1 ± 7.4 nm, respectively, for uncoated and coated cells. To further demonstrate that the LbL procedure generated a complete coating on cell surfaces, positively charged, amine-functionalized latex beads were used as a last layer in the coating

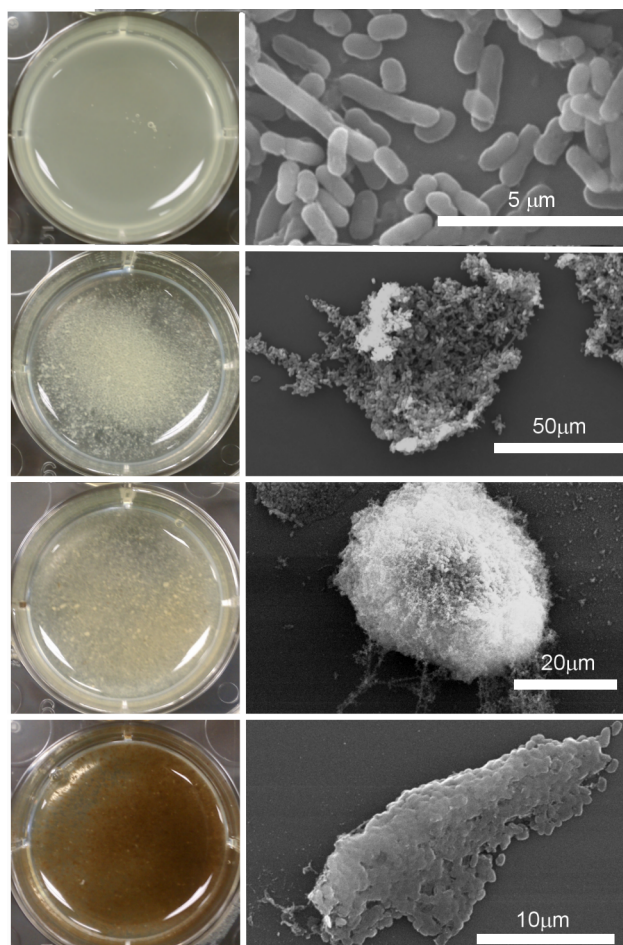


Figure 3. Cell suspensions in microplate wells (left) and SEM images (right) of uncoated cells (top) and cells coated with PAH and PVS, PSS, and HA (under uncoated from top to bottom, respectively).

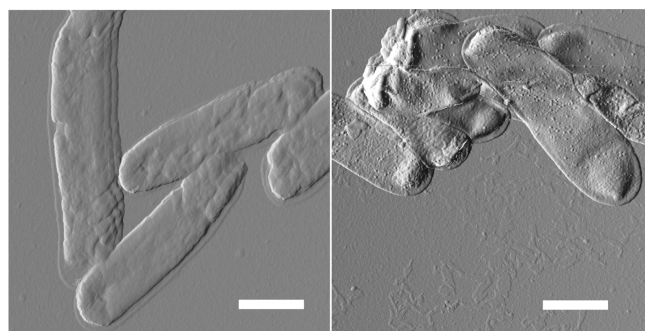


Figure 4. Typical AFM images of uncoated cells and coated cells. R34(pGFPuv) cells are shown uncoated (left) and coated with 2 layers of PAH and PSS each (right). Scale bars = 200 nm. Images show amplitude error, which provides high-resolution details and edge enhancement of cell surfaces, but does not show height.^{37,38} Corresponding height images are shown in the Supporting Information.

procedure (see the Supporting Information). SEM images show a uniform coating of 100 nm mean diameter beads on coated cells with an anionic polyelectrolyte as the outermost layer and on the negatively charged surfaces of uncoated cells.

Sensitivity to UV radiation was determined three ways: protein stability by GFPuv fluorescence intensity, the metabolic state of cells by measuring the relative intracellular ATP

concentration, and cell viability by CFU enumeration (Figure 5). GFPuv fluorescence steadily declined over the course of the experiment for coated cells, but not as rapidly as the reduction in fluorescence recorded for uncoated cells. The relative ATP concentration measured through the luminescence assay showed variation among cells with different coatings. ATP levels in cells coated with PSS and HA increased in the first 20 and 60 min, respectively, and then slowly declined at similar rates for the remainder of the assay. PVS-coated cells exhibited a 20% decrease in ATP levels in the first 15 min and then decreased at a rate similar to PSS- and HA-coated cells. ATP levels in

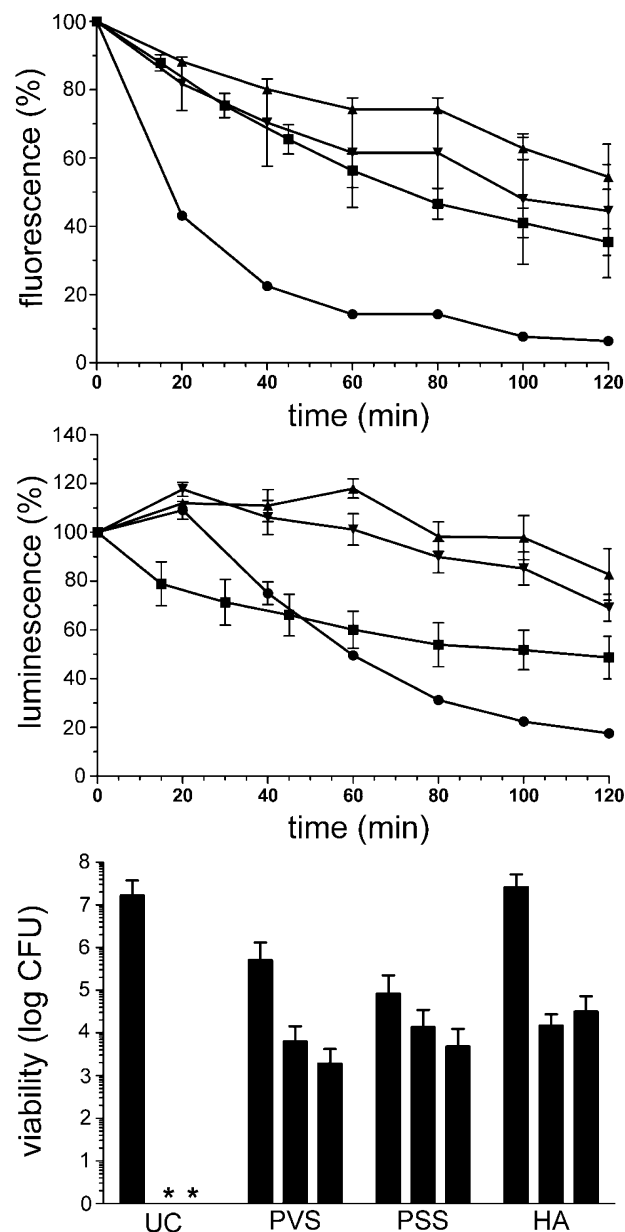


Figure 5. Relative GFP fluorescence (A), relative ATP concentration measured by luminescence (B), and viability (C) of uncoated (●, UC) and coated cells during UV exposure. Coated cells contained two layers each of PAH and PVS (■), PSS (▼), or HA (▲). Viability was measured prior to exposure (left bar in each group) and after 60 min (middle) and 120 min (right). Asterisk denotes that no colonies grew when 100 μL of the culture was plated to solid media and incubated overnight at 37 °C.

uncoated cells increased in the first 20 min, but a rapid decline in ATP occurred between 20 and 120 min. At the end of 120 min, uncoated cells had lost more than 90% of initial concentration of intercellular ATP, while coated cells retained at least 50% of their ATP concentrations. There was no significant difference in ATP concentration between the start and the end of the assay for HA-coated cells, suggesting strong UV protection with HA coatings.

Uncoated cells were unable to reproduce after 60 min exposure to UV radiation (>7 log dead), while coated cells lost viability after UV exposure, but a fraction were able to grow after plating on solid nutrient media. A variation in viable counts between cell suspensions at the start of the assay was observed, even though cell preparation and coating methods were designed to normalize cell number in assay conditions. While different cell concentrations were calculated in the cell suspension at the start of the assay, ATP levels in all cell suspensions at the beginning of the assay were within 1 order of magnitude of each other, suggesting that cell concentrations of coated and uncoated cells were not as varied as the measured CFU counts. The differences in CFU counts between cell suspensions at the start of the assay is most likely due to the aggregation properties of coated cells and not to different initial cell concentrations. The images in Figure 3 support that lower CFU counts at the start of the assay for PSS- and PVS-coated cells were due to aggregated cells. Hence, an aggregate of cells produced one CFU, leading to lower CFU counts at the start of the assay. The degree of aggregation is different for the different coatings. For example, HA-coated cells did not aggregate to the extent of cells coated with PSS and PVS (as shown in the SEM image in Figure 3). As such, CFU counts at the start of the assay for HA-coated cells were comparable to those of uncoated cells.

Activity and UV Sensitivity of Coated Riboswitch Biosensors. The riboswitch biosensor strain BL21-(pSAL:RS12.1GFPa1His) was adsorbed onto microplate well surfaces and coated with successive layers of PAH and anionic polyelectrolyte. SEM imaging revealed that single cells were adsorbed and dispersed randomly on microplate well surfaces (see the Supporting Information). We assessed the ability of coated and uncoated cells to interact with the target molecule theophylline and in response, express GFPa1. Table 1 summarizes the V_{\max} of GFP expression, time at V_{\max} ($t_{V\max}$), lag time (t_{lag}), and fold RFU increase at $t_{V\max}$ ($\text{RFU}_{V\max}/\text{RFU}_0$) for each of the experimental trials. Cells coated with PSS exhibited the highest rate of GFPa1 expression as well as the largest fold increase in GFPa1 fluorescence over baseline fluorescence. While the GFPa1 expression and fluorescence of uncoated cells and cells coated with PVS and HA were comparable, the time required to induce GFPa1 expression was

Table 1. Kinetics of Uncoated and Coated Riboswitch Biosensor Cells

cells ^a	V_{\max} (RFU min ⁻¹)	$t_{V\max}$ (min)	t_{lag} (min)	$\text{RFU}_{V\max}/\text{RFU}_0$
UC	20.5 ± 11.0	710 ± 104	470 ± 140	2.24 ± 0.28
PVS	21.7 ± 7.7	675 ± 34	409 ± 59	2.23 ± 0.59
PSS	59.3 ± 18.2	487 ± 34	311 ± 41	3.12 ± 0.71
HA	33.7 ± 9.3	345 ± 44	172 ± 22	1.89 ± 0.35

^aCells are uncoated (UC) or coated with two layers each of PAH and the listed anionic polyelectrolyte. See text for explanation of variables and data.

considerably different. Cells coated with PSS and HA exhibited the shortest time to maximal GFPa1 expression and minimal lag time. Cells coated with PVS were not statistically different from uncoated cells in all measured kinetic properties.

Coated and uncoated cells were exposed to UV radiation and expression of GFPa1 was monitored by fluorescence (Figure 6).

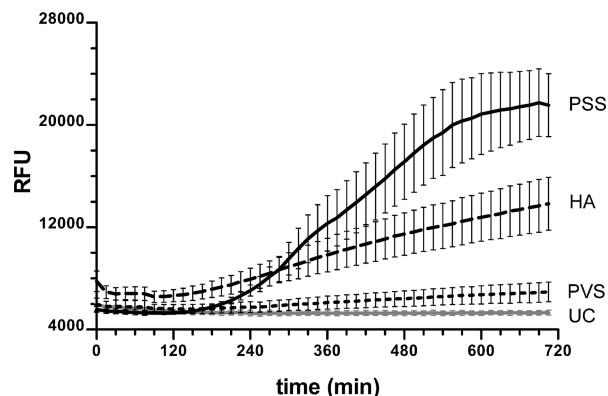


Figure 6. Fluorescence of riboswitch biosensor cells uncoated (gray) and coated with PVS (dotted line), PSS (solid line), and HA (dashed line).

Cells coated with either PSS or HA expressed GFPa1 in response to the theophylline, while no significant increase in fluorescence was observed for PVS-coated and uncoated cells. The kinetic analysis as reported in Table 1 was completed for PSS- and HA-coated cells (Table 2). Time of induction and

Table 2. Kinetics of Coated Riboswitch Biosensor Cells During UV Exposure

cells ^a	V_{\max} (RFU min ⁻¹)	$t_{V\max}$ (min)	t_{lag} (min)	$\text{RFU}_{V\max}/\text{RFU}_0$
PVS	3.3 ± 1.6 ^b	NC ^c	NC	NC
PSS	47.0 ± 19.5	410 ± 57	224 ± 33	2.33 ± 0.76
HA	15.9 ± 6.6	300 ± 26	156 ± 21	1.23 ± 0.15

^aCells are coated with two layers each of PAH and the listed anionic polyelectrolyte. See text for explanation of variables and data. ^bAverage rate (RFU min⁻¹) and not V_{\max} . ^cNot calculated.

expression rates of PSS- and HA-coated cells were similar to expression rates of the cells when not exposed to UV. V_{\max} and $\text{RFU}_{V\max}/\text{RFU}_0$ were slightly reduced, yet $t_{V\max}$ and t_{lag} were slightly increased. Kinetic data for uncoated and most of the PVS-coated cell variables was not calculated because GFP expression in response to theophylline was not sufficient.

DISCUSSION

Effect of UV-Absorbing Polyelectrolyte Coatings on the UV Sensitivity of Cells. The study tested the ability for three different anionic polyelectrolyte coatings to absorb UV radiation and mitigate harmful effects to cells. PAH does not absorb light in the UV range. PVS and PSS have similar absorption spectra at 254 nm (UVC), but PSS also absorbs significantly in the far UV region. HA has a broad absorbance throughout the UV range. For cells expressing GFPuv, the application of UV-absorbing polymer coats had a significant effect on the ability of cells to maintain GFPuv stability and metabolic activity during exposure to the germicidal lamp. Mercury vapor lamps common to germicidal UV irradiation systems emit light in a narrow bandwidth centered at 254 nm,

which acts as a potent mutagen to break DNA molecular bonds and thereby significantly reducing growth and reproduction.³⁹ UV radiation also photosensitizes intracellular O₂ to form singlet oxygen, which will react with amino acid side chains and reduce protein stability. GFPuv is excited by long-wave UV and requires ionization for fluorescence, but is still susceptible to short-wave UV-generated oxyradical damage.⁴⁰ The detrimental effects of UV radiation on protein stability, metabolic rate, and, in particular, viability were observed in uncoated cells. In contrast, the coated cells fared much better during UV exposure, because each anionic polyelectrolyte absorbs light effectively at 254 nm. When different coatings are compared, cells coated in PVS were the most sensitive to UV light. PSS and HA are polyaromatic, which provides excellent absorption in the UV range and is likely why these polymers provide better protection to cells than PVS.

Effect of Polyelectrolyte Coatings on Riboswitch Biosensor Response and UV Protection. The kinetics of biosensor response were first assessed in order to determine the expression level of each type of coated cell prior to UV exposure. As Table 1 shows, the time at which the riboswitch responds to theophylline and the rate at which GFPa1 is expressed are dependent on the specific coating. Overall, PSS- and HA-coated cell exhibited the best biosensor response, demonstrating a higher response rate and faster response time than the PVS-coated and uncoated cells. PSS and HA contain aromatic groups, and hydrophobic interactions between theophylline and the aromatic groups of PSS and HA (e.g., π - π stacking) may promote accumulation of theophylline on the surface of PSS- and HA-coated cells.¹⁸ The attraction between coating and theophylline may enhance target transfer into the cell and result in a shorter lag time to GFPa1 expression. The shortest time for GFPa1 expression (t_{Vmax} and t_{lag}) was recorded for HA-coated cells; albeit, these cells did not exhibit the highest rate of expression (V_{max}), which was measured for PSS-coated cells. It is currently unknown why HA and PSS coatings cause these differences in the kinetic data, but may be attributed to how theophylline interacts with each coating and its rate of translocation through the coating and across the cell membrane.

The biosensor function of PSS- and HA-coated cells was relatively unaffected by UV radiation; the GFPa1 expression rate and max fluorescence was only modestly reduced after exposure to UV light. As expected, UV light completely disrupted the response from uncoated cells. Surprisingly, the response to theophylline in PVS-coated cells was also significantly disrupted. In the previous set of experiments, PVS coatings protected *E. coli* (pGFPuv) from UV damage. Therefore, we assumed that the protection would also be present when biosensor cells were adsorbed to microwell plate surfaces. The difference in the protective qualities might be attributed to the aggregation of *E. coli* (pGFPuv) cells when in suspension. In Nature, cells aggregate to protect against harsh conditions and extreme variations in the environment. Cells exposed on the surface of the aggregate will be susceptible and are sacrificed, while cells within the aggregate are more protected and remain viable. This is a common property of biofilms and other cell populations that exist in a community. PVS-coatings caused *E. coli* (pGFPuv) cells to aggregate in solution, thus providing an additional mechanism for UV protection. In the microplate experiments, cells were immobilized to well surfaces and did not have an opportunity to aggregate during or after the coating procedure and PVS

coatings alone were not sufficient for UV protection. As such, the ability of the LbL coatings to induce aggregation can be an advantage to biosensor resilience. Whole-cell biosensors will likely operate with improved sustainability and resilience as aggregates, and this characteristic should be addressed in the design of biosensor material based on bacteria.

CONCLUSIONS

This work demonstrates that LbL polyelectrolyte coatings can be used to coat whole-cell sensors and endow specific properties to the cell. The LbL process is benign and retains cellular function and viability. On the basis of the polyelectrolyte characteristics, materials can be tuned to enhance biosensor function and properties. The polyelectrolyte used affects the kinetics of target interaction with biosensor and reporting function. The aromatic anionic polyelectrolytes provide excellent protection against UV radiation, allowing cells to retain biosensing functions and remain metabolically active and viable after prolonged exposure to UVC radiation from a germicidal lamp.

ASSOCIATED CONTENT

Supporting Information

AFM height images and measured cell edges of uncoated and coated cells and SEM images of latex bead coated cells and cells adsorbed to microplate well surfaces. This material is available free of charge via the Internet at <http://pubs.acs.org>.

AUTHOR INFORMATION

Corresponding Author

*Telephone: 850-283-6023. Fax: 850-283-6090, E-mail: (D.M.E.) donald.eby.ctr@us.af.mil; (G.R.J.) glenn.johnson.8@us.af.mil.

Notes

The authors declare no competing financial interest.

ACKNOWLEDGMENTS

We acknowledge the generous contribution of Prof. Dimitri Deheyn of Scripps Institution of Oceanography, University of California, San Diego for the GFPa1 gene. Work presented herein was supported by funding from the Air Force Office of Scientific Research, the Material and Manufacturing Directorate, and the 711th Human Performance Wing, Human Effectiveness Directorate, Air Force Research Laboratory.

REFERENCES

- (1) Gao, Q.; Garcia-Pichel, F. Microbial Ultraviolet Sunscreens. *Nat. Rev. Micro.* **2011**, *9*, 791–802.
- (2) Seckbach, J.; Pattanaik, B.; Schumann, R.; Karsten, U. Effects of Ultraviolet Radiation on Cyanobacteria and their Protective Mechanisms. In *Algae and Cyanobacteria in Extreme Environments*, Seckbach, J., Ed.; Springer: Netherlands, 2007; pp 29–45.
- (3) Siezen, R. J. Microbial Sunscreen. *Microb. Biotechnol.* **2010**, *4*, 1–7.
- (4) Plonka, P. M.; Grabacka, M. Melanin Synthesis in Microorganisms - Biotechnological and Medical Aspects. *Acta Biochim. Pol.* **2006**, *53*, 429–443.
- (5) Elasm, M. O.; Miller, R. V. Study of the Response of a Biofilm Bacterial Community to UV Radiation. *Appl. Environ. Microbiol.* **1999**, *65*, 2025–2031.
- (6) Su, L.; Jia, W.; Hou, C.; Lei, Y. Microbial Biosensors: A Review. *Biosens. Bioelectron.* **2010**, *26*, 1788–1799.
- (7) Hockberger, P. E. The Discovery of the Damaging Effect of Sunlight on Bacteria. *J. Photochem. Photobiol. B* **2000**, *58*, 185–191.

- (8) Reed, R. H. The Inactivation of Microbes by Sunlight: Solar Disinfection as a Water Treatment Process. *Adv. Appl. Microbiol.* **2004**, *54*, 333–365.
- (9) Detzel, C. J.; Larkin, A. L.; Rajagopalan, P. Polyelectrolyte Multilayers in Tissue Engineering. *Tissue Eng. Part B Rev.* **2011**, *17*, 101–113.
- (10) Semenov, O. V.; Malek, A.; Bittermann, A. G.; Voros, J.; Zisch, A. H. Engineered Polyelectrolyte Multilayer Substrates for Adhesion, Proliferation, and Differentiation of Human Mesenchymal Stem Cells. *Tissue Eng. Part A* **2009**, *15*, 2977–2990.
- (11) Balkundi, S. S.; Veerabadran, N. G.; Eby, D. M.; Johnson, G. R.; Lvov, Y. M. Encapsulation of Bacterial Spores in Nanoorganized Polyelectrolyte Shells. *Langmuir* **2009**, *25*, 14011–14016.
- (12) Fakhrullin, R. F.; Zamaleeva, A. I.; Morozov, M. V.; Tazetdinova, D. I.; Alimova, F. K.; Hilmudinov, A. K.; Zhdanov, R. I.; Kahraman, M.; Culha, M. Living Fungi Cells Encapsulated in Polyelectrolyte Shells Doped with Metal Nanoparticles. *Langmuir* **2009**, *25*, 4628–4634.
- (13) Franz, B.; Balkundi, S. S.; Dahl, C.; Lvov, Y. M.; Prange, A. Layer-by-Layer Nano-Encapsulation of Microbes: Controlled Cell Surface Modification and Investigation of Substrate Uptake in Bacteria. *Macromol. Biosci.* **2010**, *10*, 164–172.
- (14) Veerabadran, N. G.; Goli, P. L.; Stewart-Clark, S. S.; Lvov, Y. M.; Mills, D. K. Nanoencapsulation of Stem Cells within Polyelectrolyte Multilayer Shells. *Macromol. Biosci.* **2007**, *7*, 877–882.
- (15) Diaspro, A.; Silvano, D.; Krol, S.; Cavalleri, O.; Gliozzi, A. Single Living Cell Encapsulation in Nano-Organized Polyelectrolyte Shells. *Langmuir* **2002**, *18*, 5047–5050.
- (16) Krol, S.; Nolte, M.; Diaspro, A.; Mazza, D.; Magrassi, R.; Gliozzi, A.; Fery, A. Encapsulated Living Cells on Microstructured Surfaces. *Langmuir* **2004**, *21*, 705–709.
- (17) Yang, S. H.; Kang, S. M.; Lee, K.-B.; Chung, T. D.; Lee, H.; Choi, I. S. Mussel-Inspired Encapsulation and Functionalization of Individual Yeast Cells. *J. Am. Chem. Soc.* **2011**, *133*, 2795–2797.
- (18) Zhang, H.-M.; Chen, T.-T.; Zhou, Q.-H.; Wang, Y.-Q. Binding of Caffeine, Theophylline, and Theobromine with Human Serum Albumin: A Spectroscopic Study. *J. Mol. Struct.* **2009**, *938*, 221–228.
- (19) Ai, H.; Fang, M.; Jones, S. A.; Lvov, Y. M. Electrostatic Layer-by-Layer Nanoassembly on Biological Microtemplates: Platelets. *Biomacromolecules* **2002**, *3*, 560–564.
- (20) Hillberg, A. L.; Tabrizian, M. Biorecognition Through Layer-by-Layer Polyelectrolyte Assembly: In Situ Hybridization on Living Cells. *Biomacromolecules* **2006**, *7*, 2742–2750.
- (21) Mansouri, S.; Merhi, Y.; Winnik, F. M.; Tabrizian, M. Investigation of Layer-by-Layer Assembly of Polyelectrolytes on Fully Functional Human Red Blood Cells in Suspension for Attenuated Immune Response. *Biomacromolecules* **2011**, *12*, 585–592.
- (22) Harbaugh, S.; Kelley-Loughnane, N.; Davidson, M.; Narayanan, L.; Trott, S.; Chushak, Y. G.; Stone, M. O. FRET-based Optical Assay for Monitoring Riboswitch Activation. *Biomacromolecules* **2009**, *10*, 1055–1060.
- (23) Suess, B.; Fink, B.; Berens, C.; Stentz, R. G.; Hillen, W. A. Theophylline Responsive Riboswitch Based on Helix Slipping Controls Gene Expression In Vivo. *Nucleic Acids Res.* **2004**, *32*, 1610–1614.
- (24) Lynch, S. A.; Gallivan, J. P. A Flow Cytometry-based Screen for Synthetic Riboswitches. *Nucleic Acids Res.* **2009**, *37*, 184–192.
- (25) Bomati, E. K.; Manning, G.; Dehey, D. D. Amphioxus Encodes the Largest Known Family of Green Fluorescent Proteins, which have Diversified into Distinct Functional Classes. *BMC Evolutionary Biol.* **2009**, *9*, 77.
- (26) Schwalbe, H.; Buck, J.; Fürtig, B.; Noeske, J.; Wöhnert, J. Structures of RNA Switches: Insight into Molecular Recognition and Tertiary Structure. *Angew. Chem., Int. Ed.* **2007**, *46*, 1212–1219.
- (27) Chavez, J. L.; Lyon, W.; Kelley-Loughnane, N.; Stone, M. O. Theophylline Detection Using an Aptamer and DNA-Gold Nanoparticle Conjugates. *Biosens. Bioelect.* **2010**, *26*, 23–28.
- (28) Jin, Y.; Huang, J.-D. Engineering a Portable Riboswitch-LacP Hybrid Device for Two-Way Gene Regulation. *Nucleic Acids Res.* **2010**, *39*, 131.
- (29) Jin, Y.; Watt, R. M.; Danchin, A.; Huang, J.-D. Use of a Riboswitch-Controlled Conditional Hypomorphic Mutation to Uncover a Role for the Essential *csrA* Gene in Bacterial Autoaggregation. *J. Biol. Chem.* **2009**, *284*, 28738–28745.
- (30) Seeliger, J. C.; Topp, S.; Sogi, K. M.; Previti, M. L.; Gallivan, J. P.; Bertozzi, C. R. A Riboswitch-Based Inducible Gene Expression System for Mycobacteria. *PLoS ONE* **2012**, *7*, 29266.
- (31) Ogawa, A. Rational Design of Artificial Riboswitches Based on Ligand-Dependent Modulation of Internal Ribosome Entry in Wheat Germ Extract and their Applications as Label-Free Biosensors. *RNA* **2011**, *17*, 478–488.
- (32) Desai, S. K.; Gallivan, J. P. Genetic Screens and Selections for Small Molecules Based on a Synthetic Riboswitch That Activates Protein Translation. *J. Am. Chem. Soc.* **2004**, *126*, 13247–13254.
- (33) Sharma, V.; Nomura, Y.; Yokobayashi, Y. Engineering Complex Riboswitch Regulation by Dual Genetic Selection. *J. Am. Chem. Soc.* **2008**, *130*, 16310–16315.
- (34) Topp, S.; Gallivan, J. P. Emerging Applications of Riboswitches in Chemical Biology. *ACS Chem. Biol.* **2010**, *5*, 139–148.
- (35) Famulok, M.; Hartig, J. S.; Mayer, G. Functional Aptamers and Aptazymes in Biotechnology, Diagnostics, and Therapy. *Chem. Rev.* **2007**, *107*, 3715–3743.
- (36) Sambrook, J.; Fritsch, E. F.; Maniatis, T. *Molecular Cloning: A Laboratory Manual*, 2nd ed.; Cold Spring Harbor Laboratory: Cold Spring Harbor, NY, 1989.
- (37) Eby, D. M.; Luckarift, H. R.; Johnson, G. R. *ACS Appl. Mater. Interfaces* **2009**, *1*, 1553–1560.
- (38) Eby, D. M.; Schaeublin, N. M.; Farrington, K. E.; Hussain, S. M.; Johnson, G. R. Lysozyme Catalyzes the Formation of Antimicrobial Silver Nanoparticles. *ACS Nano* **2009**, *3*, 984–994.
- (39) Pattison, D.; Davies, M. Actions of Ultraviolet Light on Cellular Structures. In *Cancer: Cell Structures, Carcinogens and Genomic Instability*, Bignold, L. P., Ed.; Birkhäuser: Basel, 2006; pp 131–157.
- (40) Alnuami, A. A.; Zeedi, B.; Qadri, S. M.; Ashraf, S. S. Oxyradical-Induced GFP Damage and Loss of Fluorescence. *Int. J. Biol. Macromol.* **2008**, *43* (2), 182–186.